

Proximity effects and vortex dynamics in superconducting heterostructures

S J Carreira^{1,3}, V Bekeris¹, Y J Rosen^{2,4}, C Monton² and Ivan K Schuller²

¹ Departamento de Física, FCEyN, Universidad de Buenos Aires and IFIBA, CONICET, Pabellón 1, Ciudad Universitaria, 1428 Buenos Aires, Argentina.

² Department of Physics, Center of Advance Nanoscience, University of California, San Diego, 9500 Gilman Drive, La Jolla, California 92093, USA.

E-mail: sjcarreira@gmail.com

Abstract. Vortex lattice dynamics has been studied in thin Nb superconducting films sputtered on top of a dense triangular array of V dots with and without an intermediate SiO₂ insulating layer. While the insulating layer modifies only slightly the Nb film corrugation, it reduces superconducting commensurability effects (CE) substantially. This implies that superconducting commensurability is dominated by proximity effects. Moreover, the H_{C2}(T) phase diagram of the sample without an insulating layer shows a parabolic temperature dependence near T_C and critical temperature oscillations with the periodicity of the matching field. Therefore, strong proximity effects locally suppress superconductivity leading to a superconducting mesh. When the proximity effect is decreased by an insulating layer, H_{C2}(T) follows the expected linear T dependence.

1. Introduction

In recent years, the fabrication of high quality superconducting (SC) heterostructures confined to the nm scale, gave rise to the discovery of novel phenomena. The systems under study comprise mainly SC thin films with a regular array of holes [1], blind holes [2], magnetic dots [3],[4] and insulating dots [5]. In type II superconductors with an array of pinning centers, commensurability effects (CE) take place for an integer or fractional number of flux lines per unit cell [6]. This is known as a "collective" effect as is strongly dependent on mutual repulsion between vortices. Vortex pinning in a thin film containing a non-ferromagnetic array of dots has been explained as a sum of different contributions, depending on the temperature and the geometry involved: 1) the depression of the superconducting order parameter in the surrounding of the dots [7], 2) intrinsic pinning due to the random film defects [8], 3) periodic thin film corrugation and film inhomogeneity [9] and 4) filling effects due to the quantized nature of the vortices [10]. The latter, known as the Little & Parks effect [11] has been widely studied in multiple connected superconducting strips and in thin films with a regular array of pinning centers [12],[13].

We explore pinning mechanisms and CE using ac-susceptibility, in thin SC Niobium (Nb) films, sputtered on top of a dense triangular array of Vanadium (V) dots with and without a SiO₂ insulating

³ Present address : Dpto. de Materia Condensada. Centro Atómico Constituyentes. CNEA. Av. Gral Paz 1499 (1650), Buenos Aires, Argentina.

⁴ Present address: Laboratory for Physical Sciences, College Park, MD 20740, USA.

layer used to separate the V dots from the Nb film. We show that the insulating barrier modifies weakly the film corrugation and inhibits the depression of superconductivity by proximity effects. Although the superconducting-matching effects persist, the $H_{C2}(T)$ phase diagram is strongly modified. The paper is organized as follows. In Section 2 we describe the experimental details. Results and discussions are presented in Section 3. Conclusions are drawn in Section 4.

2. Experimental

A dense submicrometric triangular array of V dots, diameter $d = (70 \pm 5)$ nm and thickness $h = (50 \pm 2)$ nm with lattice parameter $D = (110 \pm 10)$ nm, was deposited on a Si substrate as described elsewhere [14]. On top of the V dots, a Nb film of thickness $\tau = (100 \pm 5)$ nm was sputtered (sample 10KC) and for the sample 10Si/V, an additional SiO_2 film of thickness $\varepsilon = (10 \pm 2)$ nm was evaporated before the Nb deposition. The bulk critical temperature of V, $T_C^{\text{V}}(\text{bulk}) = 5.4$ K [15], is lower than the bulk critical temperature of Nb, $T_C^{\text{Nb}}(\text{bulk}) = 9$ K [16]. It is well known that critical temperature may be modified for films or heterostructures [17]. In these experiments, V dots remain normal in both samples in the field and temperature ranges studied, as we found no evidence of its SC transition [18].

3. Results and discussion

Figure 1 (a) shows the zero field temperature dependence of AC susceptibility, χ' , for sample 10KC (full) and 10Si/V (open symbols). An AC magnetic field $h_{ac} = 0.25$ Oe has been applied perpendicular to the samples. The zero field critical temperatures (T_C), are $T_C^{10KC} = (6.60 \pm 0.02)$ K and $T_C^{10Si/V} = (7.17 \pm 0.02)$ K for sample 10KC and sample 10Si/V, respectively.

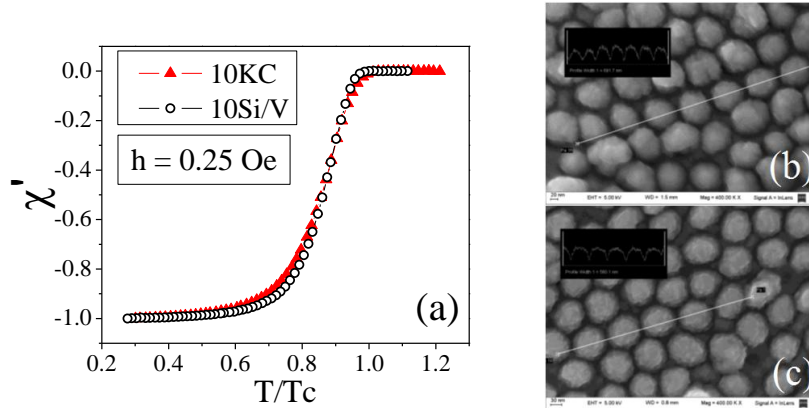


Figure 1: (a) $\chi'(T/T_C)$ ($h_{ac} = 0.25$ Oe, $H = 0$) for sample 10KC (full) and 10Si/V (open symbols). (b-c) SEM images and intensity profiles of the surface of sample 10KC (b) and 10Si/V (c).

Note the similarity between both transitions vs $t = T/T_C$. In these heterostructures, periodic surface corrugation and thickness variation of the Nb thin film around the V dots can produce CE [19]. In addition, normal V dots can depress the superconducting order parameter of the Nb thin film by proximity effects, leading to vortex pinning. Since the surface Nb corrugation and the V dots lattice have the same periodicity (in fact, one produces the other), both mechanisms may lead to the same matching fields. Consequently, it is not straightforward to assess independently the strength of each pinning mechanism.

To determine the influence of the proximity effect of V dots on the Nb thin film we measured the corrugation in samples 10KC and 10Si/V by Scanning Electron Microscopy (SEM) as shown in figure 1 (b) and (c) respectively. By comparing intensity profiles from SEM images at the same magnification, we found that the 10 nm Si layer in 10Si/V reduces the surface corrugation only by $\sim 10\%$ compared to the surface corrugation in sample 10KC. The unexpected corrugation similarities in both samples implies that differences in pinning are not related to corrugation effects.

Figure 2 (a) shows AC susceptibility measurements vs DC magnetic field, applied perpendicular to the surface of both samples in zero field cooling experiments.

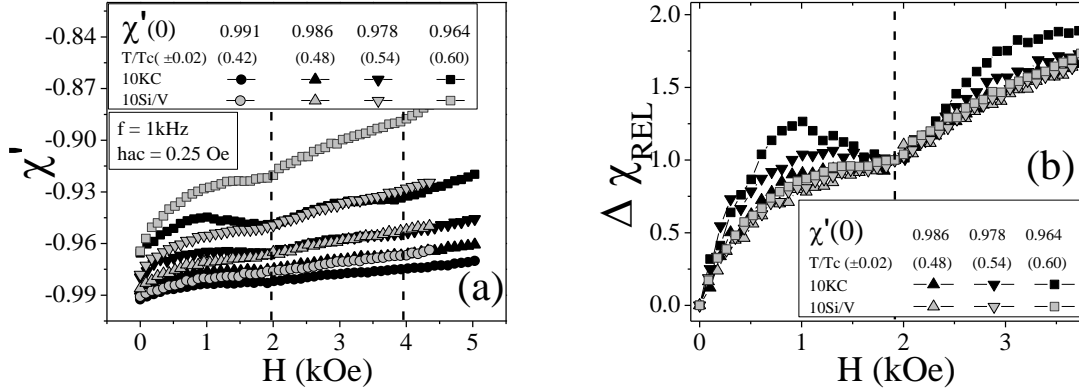


Figure 2: (a) Shielding capability vs DC magnetic field of the sample 10KC (full) and 10Si/V (open symbols). (b) $\Delta\chi_{REL} = (\chi(H) - \chi(0)) / (\chi(H_1) - \chi(0))$ extracted from data in (a). Vertical dashed lines indicate the first and second matching fields.

We compare curves at the same reduced temperature and zero field shielding capability, for the sample 10KC (full) and 10Si/V (open symbols). Vertical lines indicate the experimental first and second matching fields $H_1 = (1975 \pm 50)$ Oe and $H_2 = (3950 \pm 50)$ Oe, in agreement with calculated values for a unit cell with lattice parameter $d = 110$ nm [6].

In figure 2 (b) we plotted $\Delta\chi_{REL} = (\chi'(H) - \chi'(0)) / (\chi'(H_1) - \chi'(0))$ vs H , which shows clearly the reduction of vortex mobility at the first matching field. The weak temperature dependence of matching intensity in 10Si/V leads us to attribute the slightly reduced vortex mobility at matching fields to the periodic surface corrugation. This implies that the SiO_2 layer isolates the SC Nb film from the normal V dots, impeding the proximity effects and the depression of the SC order parameter thus reducing matching effects. In contrast, CE are clearly enhanced and temperature dependent for the sample 10KC. Since both samples have almost the same corrugation, this implies that proximity effects between the normal V dots and Nb film in the sample 10KC, depress the SC parameter in the film around localized regions close to each V dot. The existence of proximity effects implies that the interfaces between the V dots and the Nb film are clean. In addition, at fields other than the matching fields screening appears to be more effective in 10KC than in 10Si/V. This is expected considering that not only surface corrugation but also pinning close to the V dots play an important role in sample 10KC. At the same reduced temperature, vortex dynamics are reduced and matching effects are clearly enhanced for sample 10KC in contrast to sample 10Si/V. CE at low temperatures (below $0.5T_c$) are smeared due to the enhancement of intrinsic random pinning as temperature is reduced.

When the temperature is raised close to T_c , the coherence length ξ changes substantially, which has important implication for the behavior of these films. In figure 3 (a) we plot the phase diagram $H_{c2}(T)$ for sample 10KC in full symbols, extracted from field cooling temperature dependent susceptibility measurements at different DC fields. Critical field shows strong non linear temperature dependence near T_c , on which an oscillatory variation with periodicity of the matching field is superimposed. The parabolic dependence of $H_{c2}(T)$ for SC strips of width w is well known and follows the expression:

$$H_{c2}(T_c) = \frac{\sqrt{12}\phi_0}{2\pi w\xi(T)} = \frac{\sqrt{12}\phi_0}{2\pi w\xi(0)} \left(1 - \frac{T_c(H)}{T_c}\right)^{1/2} \quad (1)$$

where $\phi_0 = 2 \times 10^{-7}$ Gcm² is the flux quantum [20].

The horizontal dashed lines indicate the first and second matching fields. As was previously discussed [21],[4], fluxoid quantization in SC wire networks gives rise to this oscillatory behavior and has been extensively studied in SC networks [12],[22], Josephson junction arrays [23], and perforated Al films [24]. These phenomena have been observed not only in SC films with an array of holes but also in films with a regular array of insulating Si dots [25], and even with magnetic dots [4],[26]. This can be understood in terms of the one-dimensional superconductivity at temperatures close to the critical temperature, when the coherence length becomes of the order or larger than the width w of the SC strips which surround the pinning centers.

In contrast, for sample 10Si/V the upper critical field, plotted in open squares in figure 3 (a), shows a linear temperature dependence and no T_C oscillations, characteristic of a continuous film with a coherence length smaller than any in-plane dimensions of the film. In this case, $\xi(0)$ was calculated using the bulk expression $H_{C2} = \phi_0/2\pi\xi^2(T)$ [20]. From the linear fit shown in dashed line in figure 3 (a), we obtain $\xi(0) = (7\pm 1)$ nm.

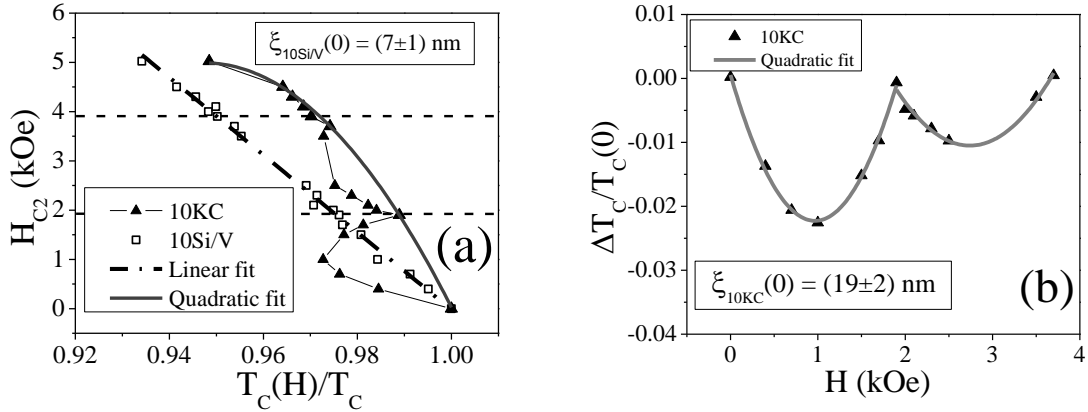


Figure 3: (a) H_{C2} vs $T_C(H)/T_C$ of the sample 10KC (full) and 10Si/V (open symbols). Solid and dash-dot lines are the quadratic and linear fittings for samples 10KC and 10Si/V respectively. Horizontal dashed lines indicate H_1 and H_2 . (b) $\Delta T_C/T_C = (T_C - T_C(H))/T_C$ vs DC field for the sample 10KC and quadratic fittings of the first two oscillations after parabolic background was subtracted.

A phenomenological model [24] used to describe the SC phase diagram of wire networks determines the oscillations with a sequence of parabolas:

$$\frac{\Delta T_C}{T_C} = -\left(\frac{\xi(0)}{d}\right)^2 \left[\frac{1}{4} - \left(\frac{\phi}{\phi_0} - n - \frac{1}{2}\right)^2 \right] \quad \Delta T_C = T_C - T_C(H) \quad (2)$$

Here, n is the number of quantum flux per unit cell, $\phi = A_{u.c.}H$ is the flux per unit cell and ΔT_C is the difference between the zero field critical temperature T_C and the critical temperature in an applied field $T_C(H)$. In terms of the lattice parameter d , the area of the unit cell for a triangular array is $A_{u.c.} = (\sqrt{3}/2)d^2$. In figure 3 (b) we plot $\Delta T_C/T_C = (T_C - T_C(H))/T_C$ vs DC field, after subtracting the parabolic background from the data in figure 3 (a). The first and second oscillations correspond to one and two flux quanta per unit cell ($n = 0$ and $n = 1$, respectively) and from (2) we estimated the G-L coherence length $\xi(0) = (19\pm 2)$ nm, which is significantly larger than the coherence length of the sample 10Si/V. The lattice parameter $d = (150\pm 40)$ nm, is in agreement with the expected value $d = 110$ nm. A parabolic fit of the data shown in figure 3 (a) to (1) together with the coherence length determined above, helps estimate the width of the SC strips, $w = (46\pm 4)$ nm. This width is smaller than the lattice parameter d . This is consistent with our geometry landscape, in which the SC strips enclose regions over the normal V dots where the Nb thin film is in the normal state.

4. Conclusions

We explored the pinning mechanisms and CE using ac-susceptibility measurements, in thin Nb films containing a dense triangular array of V dots. We compared samples with similar corrugation, with and without an intermediate insulating SiO₂ layer. Stronger matching effects occur for the sample where proximity effects induce pinning (i.e. without the SiO₂ layer). Moreover, the phase diagram H_{C2}(T) is strongly modified. Therefore, we conclude that the local depression of superconductivity in the Nb thin film by proximity effects with the V dots, is responsible for the observed T_C oscillations.

The research at UCSD was supported by the Office of Basic Energy Science, U.S. Department of Energy, BES-DMS funded by the Department of Energy's Office of Basic Energy Science, DMR under grant DE FG03 87ER-45332. Research at UBA was supported by ANPCyT grant PICT N° 753 and UBA grant UBACyT 661.

References

- [1] Berdiyrov G R, Milošević M V and Peeters F M 2006 *Phys. Rev. B* **74** 174512.
- [2] Silhanek A V, Raedts S, Van Bael M J and Moshchalkov V V 2004 *Eur. Phys. Jour. B* **37** 19.
- [3] Milošević M V, Yampolskii S V and Peeters F M 2002 *Phys. Rev. B* **66** 174519.
- [4] Gomez A, del Valle J, Gonzalez E M, Chilotte C E, Carreira S J, Bekeris V, Prieto J L, Schuller Ivan K and Vicent J L 2014 *Supercond. Sci. Technol.* **27** 065017.
- [5] Hoffmann A, Prieto P and Schuller Ivan K 2000 *Phys. Rev. B* **61** 6958.
- [6] Vélez M, Martín J I, Villegas J E, Hoffmann A, González E M, Vicent J L and Schuller Ivan K 2008 *J. Magn. Magn. Mater.* **320** 2547.
- [7] Patel U, Xiao Z L, Hua J, Xu T, Rosenmann D, Novosad V, Pearson J, Welp U, Kwok W K, and Crabtree G W 2007 *Phys. Rev. B* **76** 020508(R).
- [8] Chilotte C, Pasquini G, Bekeris V, Villegas J E, Li C-P and Schuller Ivan K 2011 *Supercond. Sci. Technol.* **24** 065008.
- [9] Lance Horng, Wu J C, Kang P C, Lin P H and Wu T C 2003 *Jpn. J. Appl. Phys.* **42** 2679.
- [10] Zhang W J *et al.* 2012 *EPL* **99** 37006.
- [11] Little W A, Parks R D 1962 *Phys. Rev. Lett.* **9** 9.
- [12] Pannetier B, Chaussy J, Rammal R and Villegier J C 1984 *Phys. Rev. Lett.* **53** 1845.
- [13] Behrooz A, Burns M J, Deckman H, Levine D, Whitehead B and Chaikin P M 1986 *Phys. Rev. Lett.* **57** 368.
- [14] Li C-P, Roshchin I V, Batlle X, Viret M, Ott F and Schuller Ivan K 2006 *J. Appl. Phys.* **100** 074318.
- [15] Sekula S T and Kernohan R H 1972 *Phys. Rev. B* **5** 904.
- [16] De Blois R W and De Sorbo W 1964 *Phys. Rev. Lett.* **12** 499.
- [17] Koren G and Millo O 2009 *Phys. Rev. B* **80** 054507.
- [18] Carreira S J, Chilotte C, Bekeris V, Rosen Y, Monton C and Schuller Ivan K 2014 *Supercond. Sci. Technol.* **27** 085007.
- [19] Jaccard Y, Martín J I, Cyrille M -C, Vélez M, Vicent J L and Schuller Ivan K *Phys. Rev. B* **58** 8232.
- [20] Tinkham M 1996 *Introduction to Superconductivity* (New York: McGraw-Hill) 2nd. edition.
- [21] Welp U, Xiao Z L, Jiang J S, Vlasko-Vlasov V K, Bader S D, Crabtree G W, Liang J, Chik H and Xu J M 2002 *Phys. Rev. B* **66** 212507.
- [22] Tinkham M *et al.* 1983 *Phys. Rev. B* **28** 6578; Wilks C W *et al.* 1991 *Phys. Rev. B* **43** 2721.
- [23] Giovannella C and Tinkham M 1995 *Macroscopic Quantum Phenomena and Coherence in Superconducting Networks* (Singapore: World Scientific).
- [24] Bezryadin A and Pannetier B 1995 *J. Low Temp. Phys.* **98** 251.
- [25] Eisenmenger J, Oettinger M, Pfähler C, Plettl A, Walther P and Ziemann P 2007 *Phys. Rev. B* **75** 144514.
- [26] Samokhvalov A V, Mel'nikov A S, Ader J-P and Buzdin A I 2009 *Phys. Rev. B* **79** 174502.